Phase Morphology and Thermomechanical Analysis of Poly(styrene-*co*-acrylonitrile)/Ethylene–Propylene–Diene Monomer Blends: Uncompatibilized and Reactively Compatibilized Blends with Two Mixing Sequences

Mona Taheri, Jalil Morshedian, Hossein Ali Khonakdar

Iran Polymer and Petrochemical Institute, P.O. Box 14965/115, Tehran, Iran

Received 9 June 2009; accepted 4 April 2010
DOI 10.1002/app.32630
Published online 18 August 2010 in Wiley Online Library (wileyonlinelibrary.com).

ABSTRACT: The phase morphology developing in immiscible poly(styrene-*co*-acrylonitrile) (SAN)/ethylene–propylene–diene monomer (EPDM) blends was studied with an *in situ* reactively generated SAN-*g*-EPDM compatibilizer through the introduction of a suitably chosen polymer additive (maleic anhydride) and 2,5-dimethyl-2,5-di-(*t*-butyl peroxy) hexane (Luperox) and dicumyl peroxide as initiators during melt blending. Special attention was paid to the experimental conditions required for changing the droplet morphology for the dispersed phase. Two different mixing sequences (simple and two-step) were used. The product of two-step blending was a major phase surrounded by rubber particles; these rubber particles contained the occluded matrix phase. Depending on the mixing sequence, this particular phase morphology could be forced or could occur spontaneously. The composition was stabilized by the formation of the SAN-*g*-EPDM copolymer between the elastomer and addition polymer, which was characterized with Fourier transform infrared. As for the two initiators, the blends with Luperox showed better mechanical properties. Scanning electron microscopy studies revealed good compatibility for the SAN/EPDM blends produced by two-step blending with this initiator. Dynamic mechanical thermal analysis studies showed that the two-step-prepared blend with Luperox had the best compatibility. © 2010 Wiley Periodicals, Inc. J Appl Polym Sci 119: 1417–1425, 2011

Key words: blends; compatibilization; morphology; reactive processing

INTRODUCTION

Polymer blending is a powerful route for obtaining materials with improved properties and cost performance. Because most blended polymers are immiscible, compatibilization is required to obtain maximum synergy. Several excellent reviews on the compatibilization of polymer blends exist.[1–8] Poly(styrene-*co*-acrylonitrile) (SAN) is a polymer without secondary relaxation processes in the main chain. Therefore, it is brittle in impact testing.[9–13] To improve this sometimes undesirable situation caused by unstable craze deformation, it is often modified with rubber particles.[14–18] Often, however, the immiscibility and incompatibility of the rubber with SAN produce poor physical properties in the blend.[19–24] A compatibilization strategy is then required to improve the physical properties. A completely different strategy for polymer blend compatibilization relies on the addition of a low-molecular-weight chemical or a mixture of low-molecular-weight chemicals. The actual compatibilizer, a branched, block, or graft copolymer, is formed during a reactive blending process.[25] This compatibilization strategy seems to be quite simple, but the lack of chemical selectivity is quite a problem.[26–30] Competition between *in situ* compatibilization, crosslinking, and degradation makes the control of blend properties very difficult. This is illustrated by the lack of convincing examples in the literature. Only when the peroxide is somehow forced to be present at the polymer interface is the chance for graft copolymer formation maximized, and this can improve the blends properties significantly. Also, some attention has been paid to the compatibilization of SAN/ethylene–propylene–diene monomer (EPDM) blends with a simple droplet morphology. In these blends, the rubber particle size plays a major role in the toughening of brittle SAN. A complex polymer blend morphology is formed in some instances. This phase structure is composed of three parts: two distinct phases with subinclusions of one phase surrounded by the other one.[31] This morphology can occur during melt processing by two-step blending. When the minor phase melts before the major phase, very small particles of the major phase can be trapped within the minor phase. This phenomenon is more often observed in reactive blends, in which the occluded particles are stabilized against

Correspondence to: J. Morshedian (j.morshedian@ippi.ac.ir).

TABLE I
Characteristic Data of the Materials

SAN	SAN-2 (Ghaed Bassir Co.)	Melt flow index = 23 g/10 min at 220°C 25–30 wt % acrylonitrile Glass-transition temperature ~ 115°C Flow temperature = 150–170°C
EPDM	Keltan 2340A (DSM Co.)	53% ethylene and 6% ENB*
Luperox	$C_{16}H_{34}O_4$	11.02% active oxygen
DCP	$C_{18}H_{22}O_2$	5.92% active oxygen
MA	$C_4H_2O_3$	Weight-average molecular weight = 98.06 Viscosity = 0.6 cP at 150°C

*Ethylene Norbornene.

coalescence by the graft copolymer in the interface.[32] This morphology can also occur in another way. An efficient strategy consists of first dispersing part of phase A within phase B and then adding large amounts of phase A (the final matrix), which triggers phase inversion.[33] The morphology of the composite dispersed phase can be stabilized by control of the viscosity of the phases and the interfacial reaction between the subinclusions and the dispersed phase.[34–37] In this study, SAN and EPDM were forced to form SAN-*g*-EPDM via the use of Luperox and dicumyl peroxide (DCP) during melt blending through the introduction of maleic anhydride (MA), which is useful for improving interfacial adhesion in blends.[38] The formation of the graft copolymer during blending with initiators resulted in a finer and more stable morphology, better adhesion between the phases of the blends, and, consequently, better properties for the final products. Effects of the annealing and mixing sequence (simple and two-step) on the blend properties were also investigated.

EXPERIMENTAL

Materials

The experiments were mainly performed with commercial products. The materials and their grades (along with the company name) are listed in Table I. Luperox [2,5-dimethyl-2,5-di-(*t*-butyl peroxy) hexane] and DCP were used as initiators. MA was used as the compatibilizing agent.

Mixing conditions

In our previous work, the effects of the initiator type and concentration and also the EPDM content on SAN/EPDM blends were studied.[30] With respect to the three initiators used, the blend prepared with 1 phr Luperox showed better mechanical properties. In this study, an EPDM concentration of 20 wt % was chosen to toughen SAN. SAN was dried *in vacuo* at 80°C for at least 12 h before the blending. Samples including EPDM, SAN, and MA were melted in a Brabender internal mixer (Lab Station, Germany) at 150°C and 60 rpm. Torque–time rheograms were analyzed for optimization. The blending for the SAN/EPDM reactive blends was conducted in two different ways:

1. Series N: EPDM (8 g) was melt-blended under the aforementioned conditions, and this was followed by the addition of SAN (32 g) and MA (1.2 g) with or without the initiator (1 phr) for 12 min. The SAN/EPDM weight composition was systematically 80/20.
2. Series S: A reactive two-step procedure included the blending of EPDM (40 g), SAN (19 g), and MA (1 g) for 8 min under moderate shear (rotor speed = 60 rpm) to prepare the EPDM master batch. Then, 12 g of the master batch was mixed with more SAN (28.2 g), MA (1 g), and initiator (1 phr) under the same blending conditions used in method I. The concentration of EPDM in the final blend was kept constant (20 wt %).

The blend compositions are summarized in Table II. NI3 and SI3 were annealed samples of NI1 and SI1, respectively; NI4 and SI4 were annealed samples of N2 and S2, respectively. The annealing was conducted for 20 min at 150°C.

Kerner model

The multiphase morphology of the blends was treated with a two-step application of the Kerner

TABLE II
Compositions of the Blends

Sample	MA	Initiator	Annealed
N1	No	No	No
S1	No	No	No
N2	Yes	No	No
S2	Yes	No	No
NI1	Yes	Luperox	No
SI1	Yes	Luperox	No
NI2	Yes	DCP	No
SI2	Yes	DCP	No
NI3	Yes	Luperox	Yes
SI3	Yes	Luperox	Yes
NI4	Yes	No	Yes
SI4	Yes	No	Yes

equation to the two-phase dispersed rubber particles. This approach was successfully used by Luzinov and coworkers[39,40] to predict the elastic moduli of ternary blends consisting of a polystyrene matrix, a styrene butadiene rubber dispersed phase, and inclusions of a polyolefin within the styrene butadiene rubber domains. Several theories have been proposed to predict the moduli of composites, and they are usually valid for binary systems consisting of the dispersion of one component in the matrix of the second component. Kerner proposed a theory for spherical dispersed phases.[41,42] In the case of ideal stress transfer across the boundary, the elastic properties are derived by the averaging of the properties of the individual components. This leads to eq. (1) for the shear storage modulus of a polyblend (E):

$$E = E_1 \frac{\dfrac{\phi_2 E_2}{(7-5v_1)E_1 + (8-10v_1)E_2} + \dfrac{\phi_1}{15(1-v_1)}}{\dfrac{\phi_2 E_1}{(7-5v_1)E_1 + (8-10v_1)E_2} + \dfrac{\phi_1}{15(1-v_1)}} \quad (1)$$

where ϕ is the volume fraction and ν is Poisson's ratio. Subscript 1 refers to the matrix, and subscript 2 refers to the dispersed phase. When no stress is transferred or when the matrix is much more rigid than the dispersed phase, the Kerner equation is simplified by the assumption that E_2 is negligible:

$$E = E_1 \frac{1}{1 + (\phi_2/\phi_1)[15(1-v_1)/(7-5v_1)]} \quad (2)$$

The inclusion of small particles (of the same chemical nature as the matrix) within the dispersed phase tends to increase the apparent volume fraction of this phase. Because the SAN matrix is much more rigid than the dispersed phase, eq. (2) predicts that an increase in the dispersed phase volume fraction will result in a lower elastic modulus. Conversely, the experimental value of the shear storage modulus can provide information on the volume fraction of the dispersed rubber phase and thus on the amount of occluded SAN.[43]

Characterization

Morphological observations

Scanning electron microscopy (SEM) was employed to characterize the blends. SEM photographs were taken of cryogenically fractured, molded, notched Izod specimens. The morphology of the fractured specimens was observed with a Cambridge S360 stereoscan electron microscope. The cryogenic specimens were dipped into liquid nitrogen for about 5 min and immediately fractured perpendicularly to the mold flow direction by hand. For better observation, the fractured specimens were etched selectively by immersion in hexane for about 6 h to remove the EPDM phase and were coated with gold before they were viewed to avoid charging. A 20-nm gold coating was used, and the coating rate was 40 mA.

Mechanical properties

Mechanical measurements of the compression-molded specimens were carried out according to ASTM D 638. The test was performed with an Instron model 6025 (High Wycombe, England) tensile testing machine with a crosshead speed of 50 mm/min at room temperature.

The Izod notched impact tests of the specimens were carried out with a pendulum-type impact tester (model 5102, Zwick, Ulm, Germany) at room temperature. At least five runs were made, and the average was reported.

Thermogravimetric analysis

The thermal stability of the polymers was investigated with a Polymer Laboratory PL-TGA apparatus. The thermogravimetric analysis was conducted in air, and the sample size was approximately 10 mg. The temperature program ranged from room temperature to complete polymer decomposition at a heating rate of 10°C/min.

Fourier transform infrared (FTIR) measurements

The structure change was studied with an FTIR spectroscopy technique. FTIR spectroscopy of SAN, EPDM, and the extracted graft copolymer was performed with an FTIR spectrometer in the transmission mode (Equinox 55, Bruker, Karlsruhe, Germany) with compression-molded thin-film samples.

Dynamic mechanical analysis

The dynamic mechanical analysis of the blends was carried out with a Tritec 2000 mechanical analyzer (Triton, London, England) operated at a fixed frequency of 1 Hz in the single-cantilever bending mode. The samples were prepared by compression molding according to ASTM E 1640. All experiments were carried out in the temperature range of −150 to 150°C at a heating rate of 5°C/min.

Rheometrics mechanical spectrometer

The rheological behavior of EPDM, SAN, N1, and S1 were studied with a parallel-plate geometry (MCR 300, Anton Paar, Graz, Austria) with a gap height of 1 mm. The dynamic measurements were carried out

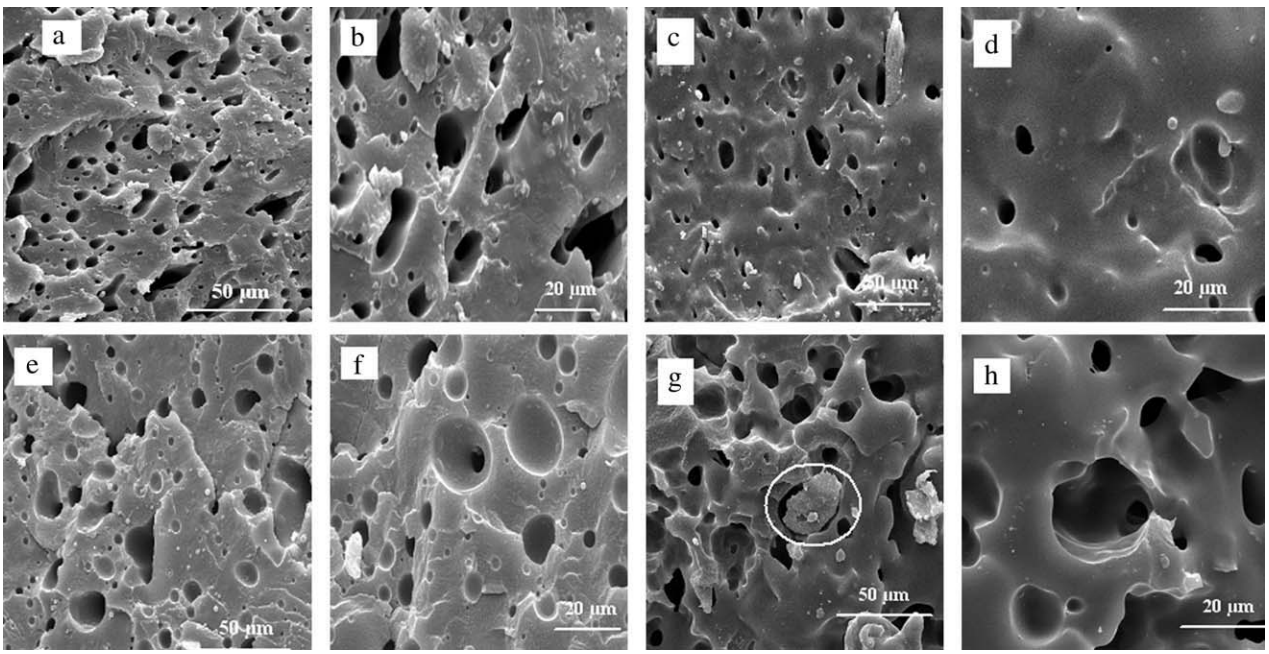

Figure 1 SEM micrographs of the blends without initiators: (a) N1 at 1000×, (b) N1 at 2000×, (c) S1 at 1000×, (d) S1 at 2000×, (e) N2 at 1000×, (f) N2 at 2000×, (g) S2 at 1000×, and (h) S2 at 2000×.

in the linear domain for frequencies ranging from 0.1 to 600 rad/s at 150°C.

RESULTS AND DISCUSSION

Effect of the mixing sequence

The inclusion of small SAN particles in the EPDM dispersed phase (SAN surrounded by EPDM in the SAN matrix to form SAN subinclusion) can be a good way of increasing the volume fraction of rubber and decreasing the interparticle distance while keeping the amount of rubber constant. The formation of subinclusions can improve the toughening properties. In the first method, SAN, MA, and the initiator were added to the melted rubber, but in the second way, they were added to the melted master batch. Figure 1 shows SEM micrographs of N1, S1, N2, and S2 blends. For N1 [Fig. 1(a,b)], a coarse droplet dispersion morphology could be observed. This type of morphology was observed for all the blends. The average radius of the dispersed phase for the S1 blend [Fig. 1(d)] was smaller than the average radius for the N1 blend [Fig. 1(b)]. However, inclusions were not formed, and the morphology did not change. Particles of different sizes were fairly uniformly distributed on the surface [Fig. 1(c,d)] and were not clearly separated into large domain sizes; this confirmed that the surface tension between the two phases was considerably reduced. The two-step blending condition resulted in better distribution and dispersion. However, it seems that with the addition of MA in the first method, rubber mobility increased, and coalescence of rubber droplets occurred; this resulted in a larger particle size for the dispersed phase [Fig. 1(e)] in comparison with N1 [Fig. 1(a)]. It seems that with the addition of SAN and MA to the master batch (S2), few inclusions were formed [Fig. 1(g)].

Figure 2 shows the storage and loss moduli with the frequency for EPDM, SAN, N1, and S1 at 150°C. At a lower frequency, the storage and loss moduli of N1 and S1 appeared between those of SAN and EPDM. The blends tended to have intermediate

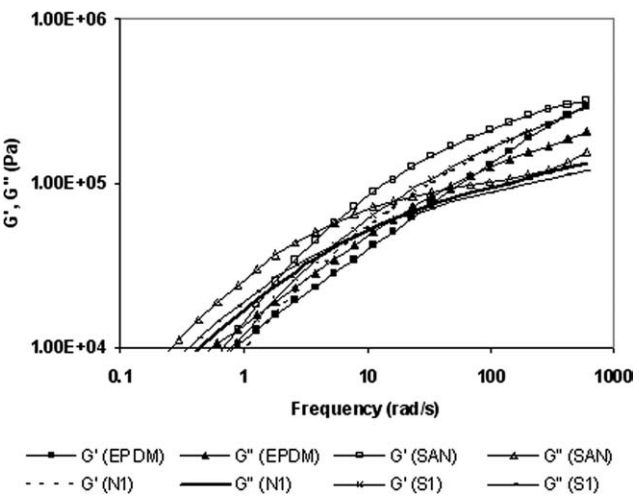

Figure 2 Storage modulus (G') and loss modulus (G'') versus the frequency for EPDM, SAN, N1, and S1 at 180°C.

properties and interchain interactions. The crossover point for S1 versus that for N1 was lower. Thus, previously observed differences in the particle size between S1 and N1 were visible by rheology.

Effect of the initiator

In the melt blending of the immiscible polymers SAN and EPDM, control of the blend morphology and the adhesion between the two polymer phases was essential for obtaining acceptable mechanical and physical properties. Two different initiators, Luperox and DCP, were used to form SAN-*g*-EPDM in the interface. The localization of the formed graft copolymer at the interface, with the block or graft extending into the respective homopolymer phases (i.e., block A in the homopolymer A phase and vice versa), not only minimized the contact between the unlike segments of the copolymer and homopolymer but also displaced the two homopolymers away from the interface and thereby decreased the enthalpy of mixing between the homopolymers.[44] Therefore, compatibility between the phases of a blend can be improved by the formation of a graft,[30] which results in better adhesion between the phases of the blend and consequently better properties for the final product.

Figure 3 shows the torque–time rheograms of the blends without an initiator (N2 and S2), with Luperox (NI1 and SI1), and with DCP (NI2 and SI2). As can be seen in the N2 and S2 rheograms, the final torque for the two-step blend (S2) was lower than that for the blend prepared by one-step blending (N2). However, with the addition of an initiator, the final torque of SI1 and SI2 increased more rapidly than that of NI1 and NI2, although the final torque of SI1 and NI1 was higher than of that SI2 and NI2. One can conclude that the amount of graft formation in the blends with DCP was lower than that in the blends with Luperox. In our previous work,[30] we showed that the concentration of the graft copolymer formed with Luperox was about 13 wt % in a blend prepared by simple blending, whereas with DCP, it was about 9 wt %.

For further explanation, the blend morphology was characterized by SEM. SEM micrographs of the blends prepared with Luperox by one-step blending (NI1) and two-step blending (SI1) and also the blends with DCP (NI2 and SI2) are depicted in Figure 4. The course of the interfacial reaction is expected to be critical in reactive processing because it should control the amount and structure of the *in situ* formed compatibilizer and thus the phase morphology and mechanical properties of polyblends. As can be seen, SI1 [Fig. 4(a)], in comparison with SI2 [Fig. 4(b)], had less SAN retention in the EPDM

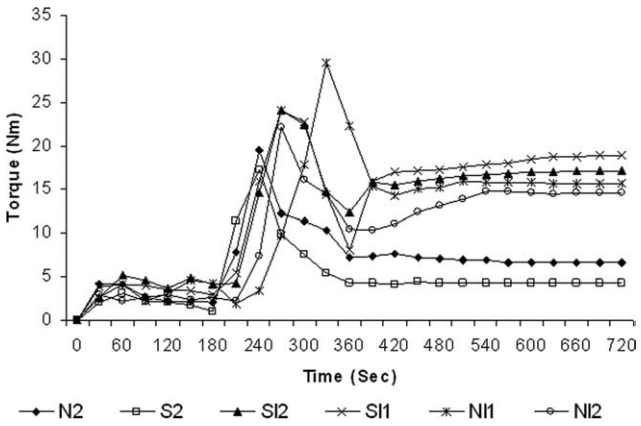

Figure 3 Torque–time rheograms of the blends.

phase. The main differences between the initiators used in this work were their active oxygen contents and their half-lives. Luperox had more active oxygen (11.02%) and a longer half-life (450 s). More active oxygen resulted in a higher amount of graft formation. The grafting rate affected not only the amount of the compatibilizer formed *in situ* but also its localization with direct consequences on the size and morphology of the dispersed rubber phase. The longer half-life led to a proper grafting rate to stabilize the complex morphology (SI1). Figure 4(c,d) presents SEM micrographs of NI1 and NI2. With the addition of the initiator, the particle size of the dispersed phase decreased, and no complex morphology was formed. As is evident from the SEM micrographs of SI1 [Fig. 4(a)] and SI2 [Fig. 4(b)], no black holes representing etched rubber particles were observed, whereas in the NI1 and NI2 micrographs, no black areas representing etched surrounding rubber were observed. The trend demonstrated in Figure 4(a,b) can be used to interpret the differences between the micrographs of Figure 1(a–d). The morphology of the sample with the initiator appeared to stabilize during heating, and the morphology did not change.

Table III shows the dependence of the shear storage modulus on the real volume fraction in series N and the apparent volume fraction in series S of the blends in different mixing sequences. The shear storage modulus of the blend and the shear storage modulus of the matrix were obtained from experimental data. Poisson's ratio of the matrix has been presented in the literature. ϕ_2/ϕ_1 can be estimated from the Kerner equation [eq. (2)]. $(\phi_2/\phi_1)_N$ represents the real volume fraction obtained from eq. (2) for series N, and $(\phi_2/\phi_1)_S$ represents the apparent volume fraction for series S. The apparent volume fraction of the EPDM minor phase was higher than the real volume fraction, which was related to the occluded SAN in EPDM. The difference between the apparent and real volume fractions was the amount of SAN occluded in the EPDM dispersed phase.

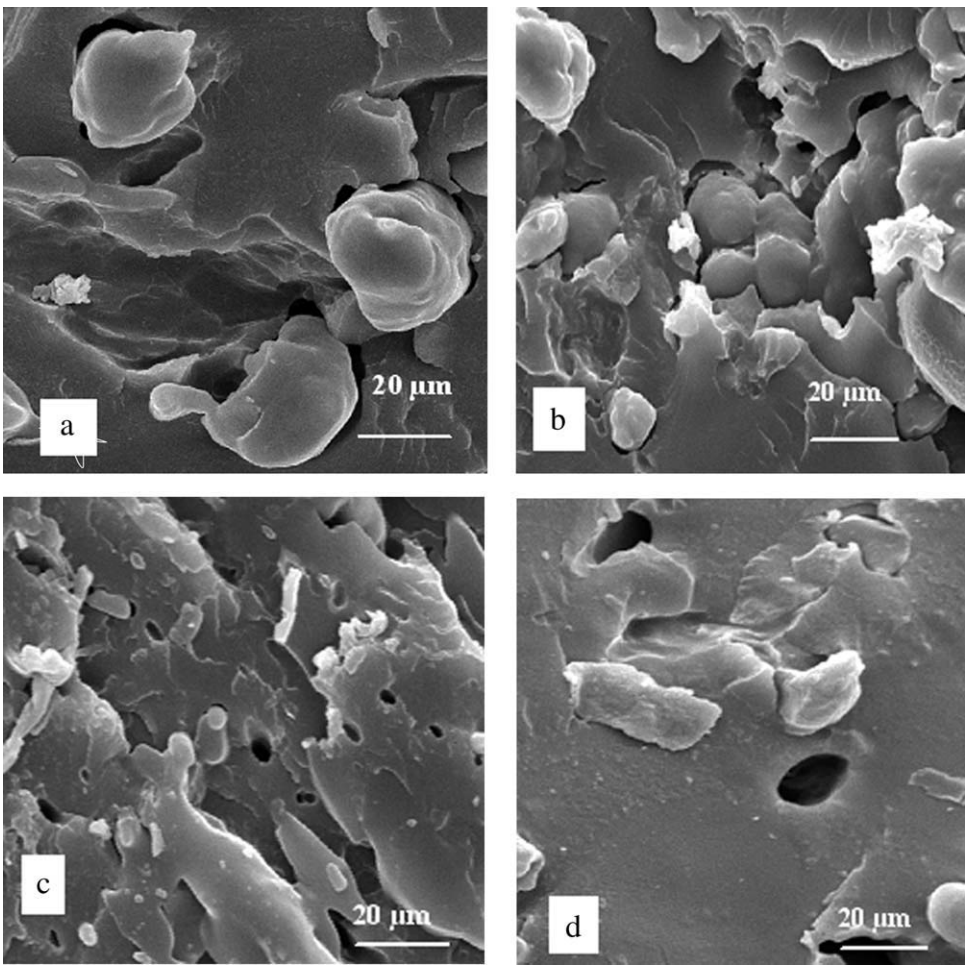

Figure 4 SEM micrographs of the blends with initiators (2000× magnification): (a) SI1, (b) SI2, (c) NI1, and (d) NI2.

This was estimated with the Kerner equation [eq. (2)] for method S (two-step blending). Density of SAN, EPDM, and ν_1 were considered to be 1.08, 0.86, and 0.35,[45] respectively.

Figure 5 shows stress–strain diagrams of the blends. With the addition of initiators to the blends (SI1 and SI2), the stress and strain at break increased. The stress and strain at break for SI1 (with Luperox) were a bit higher than those for SI2 (with DCP).

Figure 6 shows FTIR spectra of N1, S1, NI1, and SI1 blends. For EPDM, an absorption band appeared at 724 cm^{-1}, which was attributed to —CH_2 stretching. Also, a C—CH_3 stretching vibration could be observed at 1372 cm^{-1}. For SAN, the characteristic peak of the —CN group appeared at 2237 cm^{-1}. All the examined blends showed characteristic vibrations of SAN and EPDM polymers. A new vibration at 1770 cm^{-1} was attributed to carbonyl groups resulting from some oxidative degradation and related to SAN-*g*-EPDM that formed during the blending.[30]

TABLE III
Dependence of the Shear Storage Modulus and Apparent Volume Fraction in Two-Step Blending

Sample	Shear storage modulus (MPa)	$(\phi_2/\phi_1)_N$	$(\phi_2/\phi_1)_S$	Occluded SAN (vol %)
N2	1010	0.115	–	
S2	947	–	0.1557	0.031
NI1	945	0.159	–	
SI1	855	–	0.233	0.057
NI2	895	0.198	–	
SI2	884	–	0.2077	0.007

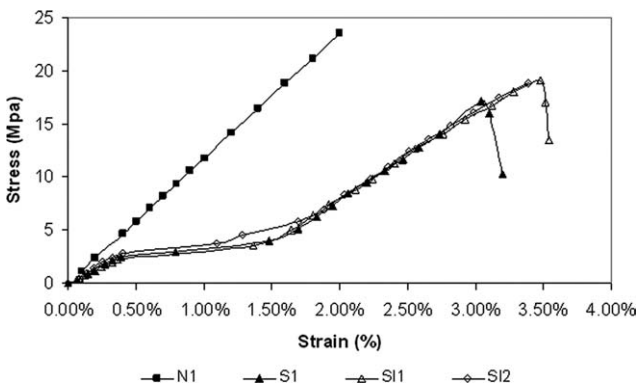

Figure 5 Effect of the initiator on the stress–strain curves of the blends.

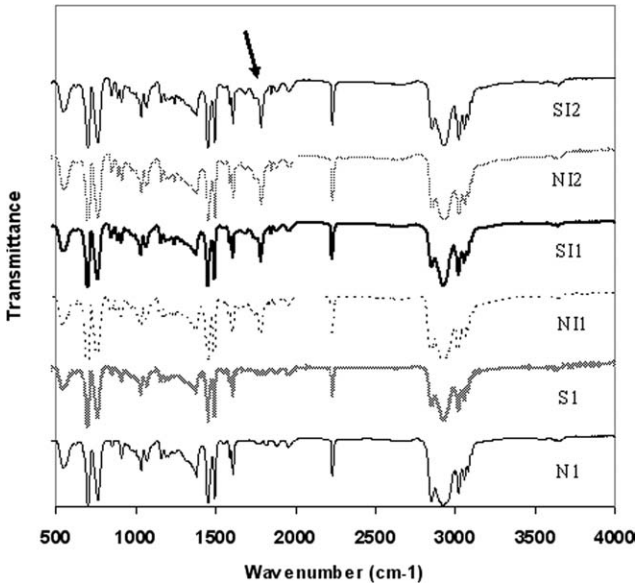

Figure 6 FTIR spectra of N1, S1, NI1, SI1, NI2, and SI2.

FTIR spectra of N1 and S1 showed no new peak. However, S1 had better mechanical properties. This could be because the morphology changed from being simple (droplet) to being complex (occluded SAN in dispersed EPDM).

Dynamic mechanical analysis

Dynamic mechanical analysis provided a clear idea about the viscoelastic properties and phase structure of the blends. Figure 7 shows tan δ, storage modulus, and loss modulus values of N1, NI1, and SI1 blends with the temperature. As can be seen in Figure 7(a), a well-defined relaxation peak was centered at 141.7°C, and it was ascribed to the glass-transition temperature of SAN in the simple SAN/EPDM blend (N1). Figure 7(b) shows the loss moduli of these blends. With the addition of an initiator, the glass-transition temperatures of SAN and EPDM moved toward each other (−45.7 and 129.7°C for N1, −41.7 and 119.6°C for NI1, and −41.7 and 115.8°C for SI1). The difference in the first peak related to the EPDM phase was less than that related to the matrix phase. The blends showed two peaks corresponding to EPDM and SAN phases. The variation of the storage modulus as a function of temperature is presented in Figure 7(c). There was a prominent increase in the modulus of SI1 at low temperatures that was related to better compatibility.

Effect of annealing

SAN is a brittle polymer. To improve this undesirable situation caused by unstable craze deformation, it is often modified with rubber particles. It is well known that in rubber-modified polymers, the impact energy can be dissipated by intensified stable crazing, which is triggered in the stress field near the rubber particles.[46] The tensile behavior of annealed samples was measured with an extensometer. Figure 8(a) shows the stress–strain behavior of the blends without Luperox. With annealing, the stiffness of the blends increased, and their toughness decreased. This was due to the decrease in the rubber mobility. The difference between the blends with MA (N2 and S2) was less than the difference between the simple blends (N1 and S1). Also, the reverse effect was observed in the blends with Luperox [Fig. 8(b)]. With annealing, the elongation at break increased, and the stiffness of the blend decreased. During annealing,

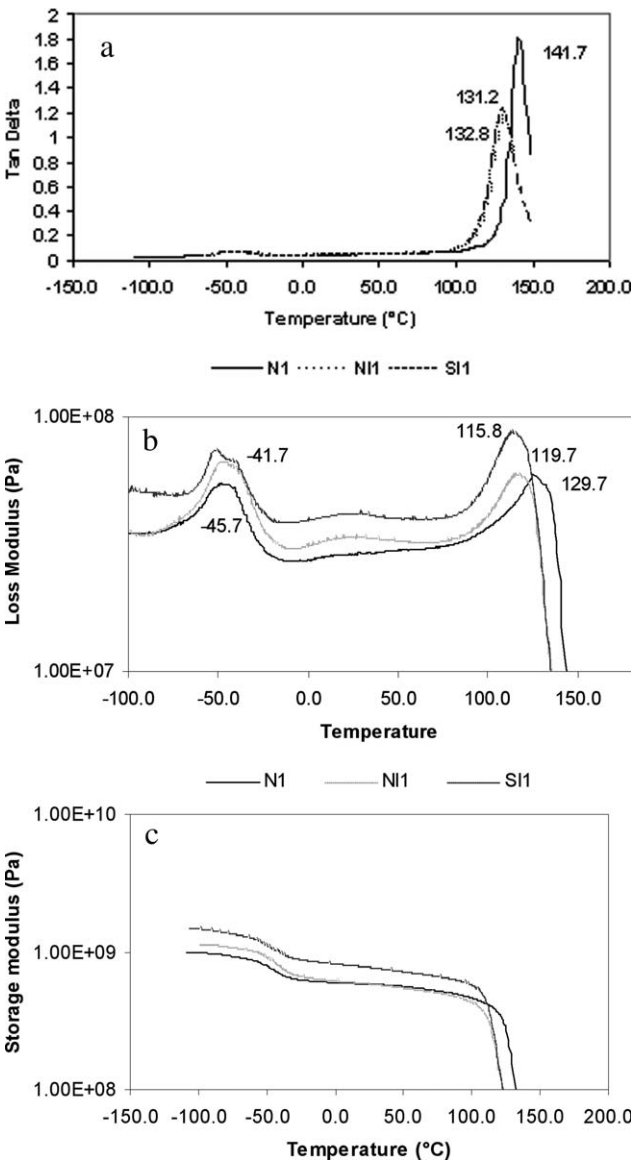

Figure 7 Dynamic mechanical behavior of N1, NI1, and SI1.

EPDM degradation occurred. The decomposition of EPDM was different in the presence of SAN. When the dispersity level of the rubber was high, the radicals forming in the EPDM phase could be transferred to the other phase to form the graft copolymer. In a reactively compatibilized blend, the morphology was stabilized and did not change during annealing. However, in an uncompatibilized blend, there was a cage effect, so gel formation increased.[30] Thermal annealing during mixing did not noticeably influence the mechanical properties of the blends prepared by two-step blending.

The mechanical properties of all the studied blends are presented in Table IV. The extensometer was used to measure the tensile behavior. By comparing the blends without initiators, we noticed that S1 had superior mechanical properties with respect to N1, but with the addition of MA, N2 showed better mechanical properties. The blends prepared with initiators by two-step blending had a higher impact strength. Annealing had a distinctive effect on the blends with and without an initiator. The blend that was prepared with Luperox and annealed showed a higher strain at break, stress at break, and impact strength. The general trend was a decrease in the modulus for the two-step blends.

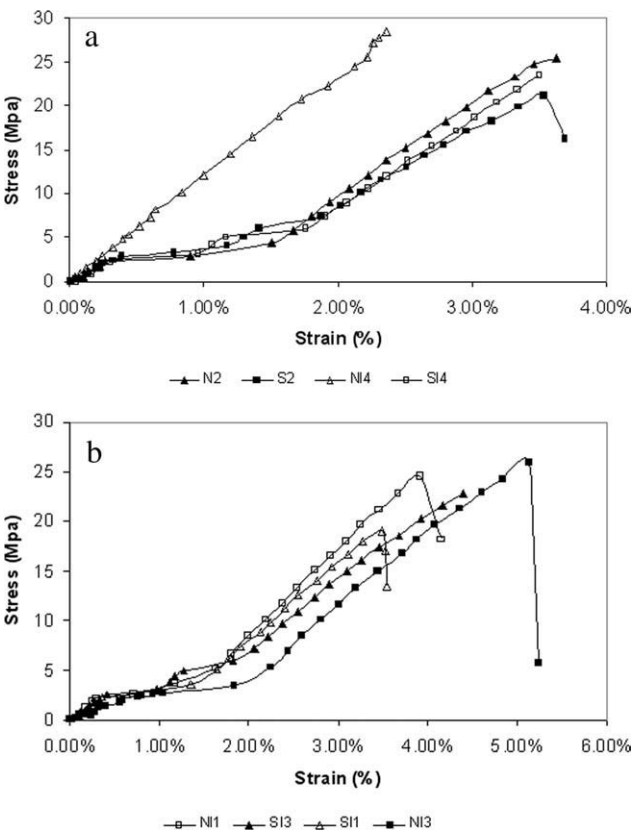

Figure 8 Effect of annealing on the stress–strain curves of the blends: (a) without Luperox and (b) with Luperox.

TABLE IV
Mechanical Properties of All Studied Blends

Sample	Impact strength (J/m)	Strain at break (%)	Stress at break (MPa)	Modulus (MPa)
N1	12.4	2.16	25.39	1175
S1	31.48	2.5	17.81	937.55
N2	16.2	2.38	25.45	1010
S2	14.3	2.67	23.05	937
NI1	17.53	3.08	26.65	945
SI1	36.57	2.35	18.9	855
NI2	12.35	1.57	11.9	895
SI2	26.2	2.44	21.01	884
NI3	18.94	3.46	25.89	891.2
SI3	42.27	2.822	20.79	795.3
NI4	11.98	2.36	29.31	1033
SI4	10.71	2.2	23.54	1034

CONCLUSIONS

Reactive blending is an efficient technique for the preparation of SAN/EPDM blends. During reactive blending, SAN-*g*-EPDM is formed, and it acts as a compatibilizer in SAN/EPDM blends. FTIR spectra showed a new peak at 1337 cm^{-1} for SAN-*g*-EPDM. We have also discussed a strategy for changing the droplet morphology to a complex morphology (small inclusions of SAN surrounded by an EPDM dispersed phase), and we have clearly shown the strong dependence of the mechanical properties on the mixing sequences and consequently on the phase morphology. The Kerner equation showed that the two-step blending method with Luperox (SI1) led to a higher apparent volume fraction ($\phi_2/\phi_1 = 0.233$). Comparing the results for all the studied blends, we can conclude that the best properties were obtained for blends prepared with Luperox with the two-step blending procedure (SI1). On the basis of the dynamic mechanical behavior, SI1 had a higher modulus and less difference in the glass-transition temperatures of SAN and EPDM (145.6°C) versus an uncompatibilized blend (156.3°C). The rheological studies have revealed that with two-step blending, elastic behavior becomes more pronounced. It has been shown that annealing has a good effect on the properties of blends prepared with initiators.

References

1. Utracki, L. A. Commercial Polymer Blends; Chapman & Hall: London, 1998.
2. Sweeney, F. M. Polymer Blends and Alloys: Guide to Commercial Products; Technic: Lancaster, PA, 1988.
3. Olabisi, O.; Robeson, L. M.; Show, M. T. Polymer–Polymer Miscibility; Academic: New York, 1979.
4. Svec, P. Ser Polym Sci Technol 1989, 20.
5. Paul, D. R. In Thermoplastic Elastomers: A Comprehensive Review; Legge, N. R.; Holden, G.; Schroeder, H. E., Eds.; Hanser: New York, 1987; Chapter 12, Section 6.
6. Jerome, R.; Fayt, R.; Teyssie, P. Polym Eng Sci 1987, 27, 328.
7. Barlow, J. W.; Paul, D. R. Polym Eng Sci 1984, 24, 525.

8. Bywater, S. Polym Eng Sci 1984, 24, 104.
9. Collias, D. I.; Baird, D. G. Polym Eng Sci 1995, 354, 1178.
10. Gusler, G. M.; McKenna, G. B. Polym Eng Sci 1997, 37, 1442.
11. Kim, J. H.; Keskkula, H.; Paul, D. R. J Appl Polym Sci 1990, 40, 183.
12. Fowler, M. E.; Keskkula, H.; Paul, D. R. J Appl Polym Sci 1988, 35, 1563.
13. Dai, J.; Wang, L.; Cai, T.; Zhang, A.; Zeng, X. J Appl Polym Sci 2007, 107, 3393.
14. Ziemka, G. P. Encyclopedia of Polymer Science and Technology; Wiley-Interscience: New York, 1964; Vol. 1, p 425.
15. Keskkula, H. Encyclopedia of Polymer Science and Technology; Wiley-Interscience: New York, 1970; Vol. 13, p 398.
16. Teyssie, P.; Fayt, R.; Jerome, R. Makromol Chem Macromol Symp 1988, 16, 41.
17. Heikens, D.; Hoen, N.; Barentsen, W.; Piet, P.; Ladan, H. J Polym Sci Polym Symp 1978, 62, 309.
18. Scobbo, J.; Stoddard, G. J. U.S. Pat. 5,334,659 (1994).
19. Kang, D.; Ha, S.; Cho, W. J. Eur Polym J 1992, 28, 565.
20. Dekkers, M. U.S. Pat. 5,356,955 (1994).
21. Qu, X.; Shang, S.; Liu, G. J Appl Polym Sci 2004, 91, 1685.
22. Zeng, Z.; Wang, L.; Cai, T. J Appl Polym Sci 2004, 94, 416.
23. Hrnjak, Z.; Jelcic, Z.; Kovacevic, V.; Mlinac, M.; Jelencic, J. Macromol Mater Eng 2002, 287, 684.
24. Taheri, M.; Morshedian, J.; Esfandeh, M. J Appl Polym Sci 2008, 110, 753.
25. Koning, K.; Duin, M. V.; Pagnoulle, C. Prog Polym Sci 1998, 23, 707.
26. Liu, N. C.; Baker, W. E. Adv Polym Technol 1992, 11, 249.
27. Xanthos, X.; Dagli, S. S. Polym Eng Sci 1991, 31, 929.
28. Kratofil, L. J.; Pticek, A.; Hrnjak-Murgic, Z. J Elast Plast 2007, 39, 371.
29. Vierle, M.; Steinhauser, N.; Nuyker, O.; Obrecht, W. Macromol Mater Eng 2003, 288, 209.
30. Taheri, M.; Morshedian, J.; Esfandeh, M. Iran Polym J 2006, 15, 955.
31. Favis, B. D.; Lavallee, C.; Deredouri, A. J Mater Sci 1992, 27, 4211.
32. Sundararaj, U. Ph.D. Thesis, University of Minnesota, 1994.
33. Yamaguchi, N.; Chikanari, T. Soc Plast Ind Soc Plast Eng Conf Prepr 1990, 165.
34. Salager, J. L. Encyclopedia of Emulsion Technology; Marcel Dekker: New York, 1988; Vol. 3, Chapter 2.
35. Smith, D. H.; Lee, K. H. J Phys Chem 1990, 94, 3746.
36. Lee, K. H.; Smith, D. H. J Colloid Interface Sci 1991, 142, 278.
37. Dickinson, K. J. Colloid Interface Sci 1981, 84, 284.
38. Barra, G. M. O. J Braz Chem Soc 1999, 10, 31.
39. Luzinov, I.; Xi, K.; Pagnoulle, C. Polymer 1999, 40, 2511.
40. Luzinov, I.; Pagnoulle, C.; Jerome, R. Polymer 2000, 41, 3381.
41. Uemura, S.; Takayanagi, M. J Appl Polym Sci 1966, 10, 113.
42. Leclair, A.; Favis, B. D. Polymer 1996, 37, 4723.
43. Rousch, J. J Polym Eng Sci 1995, 35, 1917.
44. Wenchun, H.; Koberstein, J. T.; Lingelser, J. P.; Gallot, Y. Macromolecules 1995, 28, 5209.
45. Nicodemo, L.; Nicolais, L. J Mater Sci Lett 1983, 2, 5.
46. Ramsteiner, F.; Heckmann, W. Polymer 2002, 43, 5995.